

# Druggable sensors of the unfolded protein response

Dustin J Maly<sup>1\*</sup> & Feroz R Papa<sup>2-5\*</sup>

**The inability of cells to properly fold, modify and assemble secretory and transmembrane proteins leads to accumulation of misfolded proteins in the endoplasmic reticulum (ER). Under these conditions of 'ER stress', cell survival depends on homeostatic benefits from an intracellular signaling pathway called the unfolded protein response (UPR). When activated, the UPR induces transcriptional and translational programs that restore ER homeostasis. However, under high-level or chronic ER stress, these adaptive changes ultimately become overshadowed by alternative 'terminal UPR' signals that actively commit cells to degeneration, culminating in programmed cell death. Chronic ER stress and maladaptive UPR signaling are implicated in the etiology and pathogenesis of myriad human diseases. Naturally, this has generated widespread interest in targeting key nodal components of the UPR as therapeutic strategies. Here we summarize the state of this field with emphasis placed on two of the master UPR regulators, PERK and IRE1 $\alpha$ , which are both capable of being drugged with small molecules.**

In eukaryotic cells, the ER comprises interconnected networks of branching tubules and sacs that are separated from the surrounding cytosol by a lipid bilayer, the ER membrane. The ER is the first organelle of the secretory pathway and therefore serves as the entryway for over a third of all cellular proteins, including those destined for secretion to the cell exterior or insertion into the plasma membrane; in this set are proteins that ultimately will reside within the ER, the Golgi or in lysosomes<sup>1</sup>. Folding, post-translational modifications, structural maturation and assembly of all of these proteins begin in the ER, in most cases even as they are cotranslationally injected through the translocon complex into the ER. Once in the ER, these client proteins of the secretory pathway fold to their native shapes and often undergo further post-translational modifications, including glycosylation and disulfide bond formation. These folding and maturation processes are catalyzed by abundant ER-resident enzymes, which include molecular chaperones, glycosylating enzymes and oxido-reductases<sup>2,3</sup>. The ionic and electronic milieu of the ER is adapted to facilitate these reactions. Compared to the cytosol, the ER maintains, through energy expenditure, a much higher calcium concentration and a much more oxidizing redox potential<sup>4,5</sup>. Together, these enzymatic processes ensure that secretory proteins are properly folded, modified and assembled, in some cases into multiprotein complexes, within the ER before they traffic farther downstream in the secretory pathway.

Faithful folding and maturation of proteins of the secretory pathway often fails, and because many of these proteins mediate crucial signaling roles, incompletely folded forms are not tolerated by the cell. Instead, these misfolded species are disposed of by stringent quality control systems such as the ER-associated degradation (ERAD) pathway, which removes unfolded proteins from the ER to the cytosol for subsequent ubiquitylation and degradation by the 26S proteasome<sup>6,7</sup>. In some instances, this process may lead to a deficiency of important proteins, causing a loss of the function that they serve. In contrast, the accumulation of unfolded proteins in the ER can also cause gain-of-function proteotoxicity.

'Professional secretory' cells, such as  $\beta$  cells of the endocrine pancreas, seem to work near the limits of their secretory capacity and normally secrete approximately 1 million molecules of insulin every minute<sup>8</sup>. As another example, plasma cells can secrete their own

weight in antibodies every day<sup>9</sup>. Thus, such cells may routinely experience ER stress from secretory exhaustion<sup>10</sup>. As a more general concept, for any type of cell, a wide range of cellular disturbances can compromise efficiency of protein folding in the ER and lead to the accumulation of misfolded proteins within the organelle. ER stress can proceed from nutrient deprivation, hypoxia, point mutations in important secreted proteins that stabilize incomplete folding forms and loss of calcium homeostasis, which in turn may impede proper functioning of ER-resident calcium-dependent chaperones<sup>11-13</sup>. In the case of  $\beta$  cells, ER stress can result from the inability to fold the increased levels of proinsulin intermediates needed to maintain blood glucose during conditions of peripheral insulin resistance<sup>14</sup>. Also, in neurons, chronic expression of folding-defective secretory proteins can saturate the protein-folding machinery and lead to ER stress<sup>15</sup>. Under ER stress, secretory proteins start to accumulate in improperly modified and unfolded forms within the organelle. Therefore, cells have evolved sophisticated surveillance systems to sense and respond to ER stress before cell function and survival is threatened.

To properly match protein-folding capacity to secretory demand, cells constantly monitor the concentration of misfolded proteins in the ER lumen and initiate corrective responses. When misfolded proteins accumulate in the ER above a critical threshold, an ancient signal transduction pathway called the UPR, which is conserved in all eukaryotes, becomes activated. The UPR is triggered by the activation of three ER transmembrane proteins: inositol requiring enzyme 1  $\alpha$  (IRE1 $\alpha$ ), pancreatic ER kinase (PERK) and activating transcription factor 6 (ATF6)<sup>16</sup>. All three of these ER stress sensors contain an ER luminal domain that directly or indirectly senses misfolded proteins (Figs. 1-3). Luminal domain sensing of misfolded proteins leads to changes in the oligomerization state of each sensor and activation of their downstream activities, transducing a signal from the ER lumen into the cytoplasm. For IRE1 $\alpha$  and PERK, luminal domain self-association, which is the initiating step, may be prevented in unstressed cells through binding of an ER chaperone called BiP<sup>17</sup>. Furthermore, through direct binding to the luminal domain of either IRE1 $\alpha$  or PERK, misfolded or unfolded proteins may act as 'activating ligands', analogous to a wide range of extracellular ligands that activate various receptors on the plasma membrane<sup>18,19</sup>.

<sup>1</sup>Department of Chemistry, University of Washington, Seattle, Washington, USA. <sup>2</sup>Department of Medicine, University of California-San Francisco, San Francisco, California, USA. <sup>3</sup>Diabetes Center, University of California-San Francisco, San Francisco, California, USA. <sup>4</sup>Lung Biology Center, University of California-San Francisco, San Francisco, California, USA. <sup>5</sup>California Institute for Quantitative Biosciences, University of California-San Francisco, San Francisco, California, USA.

\*e-mail: maly@chem.washington.edu or frpapa@medicine.ucsf.edu

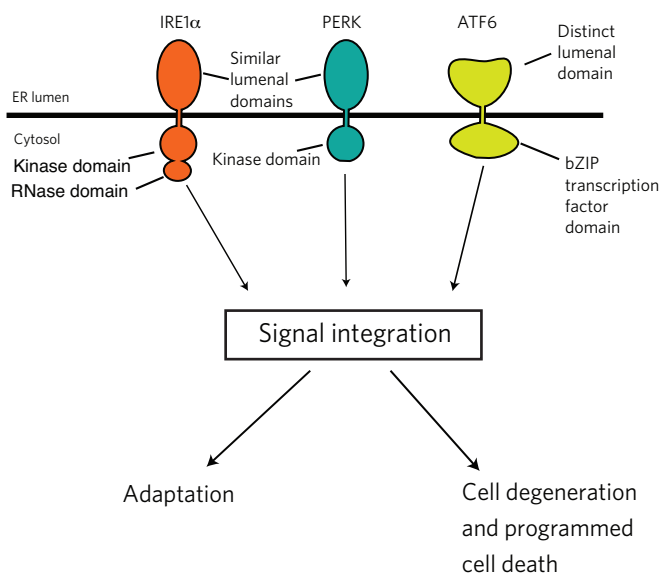


**Figure 1 | The three arms of the UPR.** Upon activation under ER stress, three sensors, IRE1 $\alpha$ , PERK and ATF6 send intracellular signals that allow the cell to either adapt or commit apoptosis.

### Activation and homeostatic signaling in the UPR

The three UPR sensors evolved outputs that initially realign protein-folding demand and protein-folding capacity, thus restoring secretory homeostasis<sup>20</sup>. This ‘adaptive UPR’ expands ER size and enhances the physiological functions of ER chaperones, oxidoreductases and ER membrane biosynthetic enzymes. Transcriptional upregulation of ERAD components by the UPR also leads to the removal and degradation of misfolded proteins from within the ER. Furthermore, transient translational blocks occur through the UPR under ER stress, which has the effect of decreasing protein flux into the secretory pathway<sup>21,22</sup>. However, through a seeming paradox, the combined outputs of the UPR can lead to various destructive outcomes, including cell proliferation blocks, dedifferentiation, inflammation and programmed cell death (typically through mitochondrial apoptosis; **Fig. 1**).

The most ancient of the UPR sensors, IRE1, exists in all eukaryotic cells. In mammalian cells, the more widely expressed of two paralogs is IRE1 $\alpha$ , which, like all IRE1 species, contains a cytoplasmic face comprising two enzymatic domains: a serine/threonine kinase domain and an endoribonuclease (RNase) domain<sup>23,24</sup> (**Fig. 2**). Upon luminal accumulation of misfolded proteins, the luminal domains multimerize, consequently juxtaposing IRE1 $\alpha$ 's kinase domains, which *trans*-autophosphorylates; this autophosphorylation event leads to conformational activation of IRE1 $\alpha$ 's RNase domain<sup>25</sup>. Upon activation, IRE1 $\alpha$ 's RNase excises a 26-nucleotide intron from the mRNA encoding the X-box protein 1 (XBP1) transcription factor. Subsequent cytosolic splicing of the two resulting mRNA fragments by an unidentified RNA ligase produces the homeostatic transcription factor XBP1s, which now contains a potent transactivation domain encoded in the altered reading frame<sup>26,27</sup>. XBP1s translocates to the nucleus and induces transcription of hundreds of genes that augment ER size and function<sup>28</sup>.

By analogy, the luminal domains of PERK (evolutionarily derived from IRE1 in higher eukaryotes) multimerize upon luminal accumulation of misfolded proteins. Similar to IRE1 $\alpha$ , the cytosolic (serine/threonine) kinase domains of PERK become *trans*-autophosphorylated, but in contrast to IRE1 $\alpha$ , for which there is currently no evidence for a subsequent protein phosphorylation cascade, activated PERK phosphorylates the eukaryotic translation

initiation factor 2 $\alpha$  (eIF2 $\alpha$ ) on its Ser51 residue<sup>29,30</sup> (**Fig. 2**). This event reduces cap-dependent translation, causing a global translational block, thus endowing the cell with an extended time window to fold preexisting proteins already present in the ER<sup>22</sup>. However, a subset of genes is granted translational privilege during the translational block imposed by PERK. For example, the mRNA encoding a transcription factor called ATF4 gains such translational privilege, and upon production of the ATF4 transcription factor, its target genes, which encode activities that increase amino acid import and glutathione biosynthesis, become induced<sup>31</sup>.

A third arm of the UPR is activated through the latent transcription factor, ATF6, which, as an ER membrane protein, trafficks in vesicles to the Golgi, where it is cleaved by site-1 and site-2 proteases to release the soluble ATF6(N) transcription factor contained on its cytoplasmic face<sup>32</sup> (**Fig. 2**). Together with XBP1s, ATF6(N) increases transcription of targets that expand the ER's size and increase its protein-folding capacity<sup>28</sup>. Thus, in aggregate, these transcriptional events combined with a transient translational block cause negative feedback loops to close as upstream ER stress becomes contained. If successful, these adaptive events promote cell survival and cause UPR signaling to wane.

### Domain architecture of IRE1 $\alpha$ and PERK

Informed by recent structural biology advances, we now delineate the mechanisms of activation of the two components of the UPR that have druggable enzymatic activity, IRE1 $\alpha$  and PERK. Full-length IRE1 $\alpha$  has an N-terminal luminal sensor domain and a cytosolic kinase–RNase domain that are connected by a type 1 transmembrane segment cytosolic linker. The canonical serine/threonine protein kinase domain and unique RNase domain of IRE1 $\alpha$  are intimately adjoined, facilitating efficient allosteric communication (**Fig. 3a**)<sup>33</sup>. The overall architecture of IRE1 $\alpha$ 's kinase domain resembles that of other protein kinases, consisting of a mainly  $\beta$ -stranded N-terminal lobe and an  $\alpha$ -helical C-terminal lobe; PERK's overall architecture is similar (**Fig. 3a**). The ATP-binding site, which contains all of the catalytic residues necessary for phosphate transfer, is located between these two lobes. The RNase domain of IRE1 $\alpha$  is rigidly fused to the C terminus of the kinase domain and is composed exclusively of  $\alpha$ -helices connected by short loops. Although IRE1 $\alpha$ 's RNase domain resembles the sterile  $\alpha$ -helix motif found in ephrin receptors, its overall fold is new and is referred to as a kinase extension RNase (KEN) domain.

Structural and biochemical studies with truncated IRE1 constructs that contain only the cytosolic RNase-kinase module have proven valuable in understanding the transition from monomer to higher-order oligomer. Numerous studies have shown that the kinase–RNase module alone (in both yeast and mammalian orthologs) is able to form dimers and oligomers that are most likely similar to the assemblies formed by full-length IRE1 tethered to the ER<sup>33–35</sup>. In the absence or ER stress, IRE1 is unphosphorylated and mainly monomeric. Indeed, analytical ultracentrifugation and cross-linking studies have shown that unphosphorylated human and yeast IRE1 kinase–RNase domain modules form very few dimers or oligomers in solution. Upon clustering under ER stress, IRE1 undergoes multiple autophosphorylation events on its activation loop and cytosolic linker, which is believed to promote dimer or oligomer formation<sup>36</sup>. This notion is supported by experiments showing that multiply phosphorylated kinase–RNase constructs form dimers or oligomers at lower concentrations in solution than the unphosphorylated forms. Thus, IRE1 autophosphorylation serves to enhance oligomer formation, which, in turn, enhances RNase activity.

Unphosphorylated human IRE1 $\alpha$  forms a dimer (face-to-face) with the ATP-binding site of each kinase domain directed toward its dimeric partner (**Fig. 3b**) in crystal structures<sup>37</sup>. The interface of the face-to-face dimer is over 1,700 Å<sup>2</sup> and is composed entirely of

residues in the kinase domain. This overall configuration results in *trans* exchange of kinase activation loops and the RNase domain of each IRE1 protomer being separated in space by over 55 Å. The face-to-face dimer of IRE1 is believed to be a stable *trans*-autophosphorylation complex that occurs at an early stage of IRE1 activation. The reduced capacity of IRE1 face-to-face dimer interface mutants to undergo autophosphorylation is consistent with this notion.

Crystal structures of yeast IRE1 in an alternative dimeric form (back-to-back) have been reported (Fig. 3b), as have those of PERK (Fig. 3b)<sup>33,35</sup>. In the back-to-back dimer, the kinase domain of each IRE1 protomer is oriented in the opposite direction than the face-to-face dimer. This brings the RNase domains of each protomer into close contact and prevents *trans* exchange of kinase activation loops. The interface of the back-to-back dimer is greater than 3,800 Å<sup>2</sup> and is composed of residues in both the kinase and RNase domains. In the back-to-back dimer, all of the catalytic residues necessary for catalyzing phosphodiester hydrolysis reside in a cleft between adjoining RNase domains. On the basis of biochemical and structural studies, a histidine and tyrosine residue that line the RNase active site are believed to serve as the general acid-base pair for catalyzing RNA cleavage. *In vitro* kinetic analysis shows that dimers and oligomers of IRE1 are the catalytically active species for RNA cleavage, and the back-to-back dimer represents the basis for assembling an active RNase. The back-to-back dimer is also able to form a scaffold required for higher-order oligomer formation.

### Terminal signaling in the UPR

If the previously described adaptive responses fail to restore protein-folding homeostasis, UPR signaling continues to persist and eventually morphs into alternate signaling programs called the terminal UPR that ultimately promote programmed cell death (Fig. 4)<sup>38</sup>. Ample evidence supports that the two UPR kinases, PERK and IRE1α, have a distinct set of proapoptotic outputs that contribute to cell degeneration and death if ER stress cannot be resolved. For example, although a temporary pause in protein translation due to eIF2α phosphorylation can be beneficial by reducing secretory load, a protracted block in translation from sustained PERK signaling is incompatible with survival. In support of this notion, temporary forced dimerization of PERK (through an FvE-PERK construct dimerized with AP20187) affords a measure of cytoprotection against subsequent exposure to ER stress in a preconditioning regime, whereas tonic PERK activation through the same maneuver promotes apoptosis<sup>39,40</sup>. In both of these instances, eIF2α phosphorylation is activated by the FvE-PERK-AP20187 inducible system. Moreover, PERK hyperactivation can upregulate the C/EBP-homologous protein (CHOP) transcription factor, which inhibits expression of the gene encoding antiapoptotic BCL-2 to hasten cell death<sup>41,42</sup>.

Similarly, when hyperactivated by chronic ER stress, phosphorylated IRE1α transitions from a homodimer into a

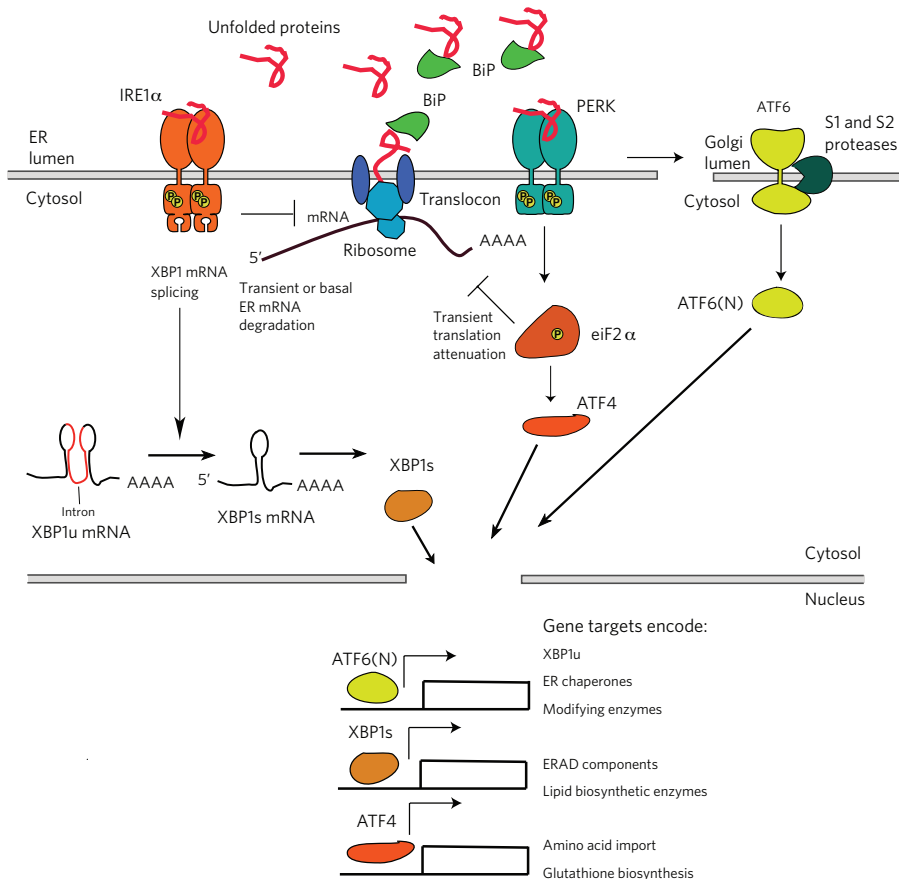


**Figure 2 | Adaptive signaling in the UPR.** Under ER stress, IRE1α's kinase domain *trans*-autophosphorylates, leading to allosteric activation of the adjacent RNase. The consequences of IRE1α phosphorylation vary depending on the level of ER stress. In response to low levels of ER stress, IRE1α's RNase excises a 26-nt intron from the mRNA encoding the XBP1 transcription factor to produce the homeostatic transcription factor XBP1s. XBP1s then translocates to the nucleus and induces transcription of many genes that attempt to restore ER homeostasis. In the presence of misfolded proteins, PERK dimerizes and phosphorylates eIF2α. Phosphorylation inhibits eIF2α activity and hence slows down global protein translation. In contrast, translation of the transcription factor ATF4 is selectively upregulated when the amount of active eIF2α is limiting. In the presence of misfolded proteins, ATF6 translocates to the Golgi and is cleaved by site-1 and site-2 proteases to release the ATF6(N) transcription factor contained within its cytoplasmic tail. Together with XBP1s, ATF6(N) increases transcription of targets that expand ER size and increase its protein-folding capacity to promote cell survival. ATF4 expression transcriptionally upregulates CHOP, which tips the ER toward homeostasis through induction of a number of corrective genes, including XBP1 and chaperones.

high-order oligomer, allowing its RNase to acquire affinity for additional RNA substrates aside from XBP1 mRNA. Under sustained oligomerization, IRE1α's RNase causes massive endonucleolytic decay of hundreds of ER-localized mRNAs containing an N-terminal signal sequence, which depletes ER cargo and protein-folding components to further worsen ER stress at later time points<sup>43,44</sup>. However, as with forced PERK activation, preemptive activation of IRE1α through chemical-genetic systems can partially prolong cell survival under ER stress. In support of this, we<sup>45</sup> and others<sup>46</sup> have demonstrated that preemptive activation of IRE1α's homeostatic arm provides a metastable degree of cytoprotection against subsequent ER stress. Owing to the highly unusual relationship between IRE1α's kinase and RNase domains<sup>47</sup>, the kinase domain of an IRE1α mutant can be engaged with an orthogonal kinase inhibitor called 1NM-PP1 to enforce an active ATP-binding conformation while bypassing autophosphorylation<sup>34</sup>, which spontaneously triggers RNase activity even without ER stress. This allosteric activation forces splicing of

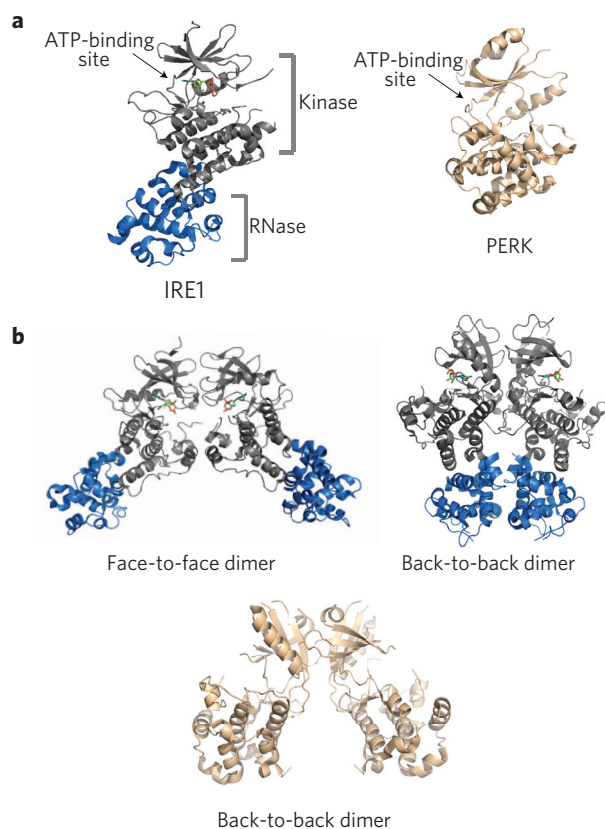


**Figure 3 | Domain architecture of IRE1 and PERK.** (a) Crystal structures of the cytosolic regions of IRE1 and PERK. Left, crystal structure of the kinase/RNase module of human IRE1 $\alpha$  (Protein Data Bank (PDB) code 3P23). The kinase domain is shown in gray, and the RNase (KEN domain) is shown in marine. The ATP-binding site of IRE1 $\alpha$  is occupied by ADP. Right, crystal structure of the cytosolic kinase domain of PERK (PDB code 4G31). (b) Crystal structures of IRE1 and PERK dimers. Left, the face-to-face dimer of human IRE1 $\alpha$  (PDB code 3P23). Right, the back-to-back dimer of yeast IRE1 (PDB code 3LJ2). Lower middle, the back-to-back dimer of PERK (PDB code 4G31).

XBP1 mRNA, resulting in the production of Xbp1. Cells subjected to these treatments preemptively are afforded a small but substantial degree of cytoprotection under ER stress<sup>45</sup>.

Although the aforementioned studies demonstrate that intermediate states are available to either PERK or IRE1 $\alpha$ , leading to divergent cell fate outcomes, IRE1 $\alpha$  oligomerization under irremediably high levels of ER stress has been shown to induce activation or upregulation of a number of proinflammatory and pro-death proteins. For example, when hyperactivated, IRE1 $\alpha$ 's RNase also reduces the levels of select microRNAs (possibly through directly cleaving their precursors at the ER membrane) that normally repress proapoptotic targets, such as pro-oxidant protein thioredoxin-interacting protein (TXNIP), leading to their rapid upregulation<sup>48,49</sup>. Increased TXNIP protein levels then activate the NLRP3 inflammasome and its caspase-1-dependent pro-death pathway, leading to sterile inflammation and pyroptotic cell death<sup>49</sup>. Finally, sustained IRE1 $\alpha$  oligomerization may serve as an activation platform for apoptosis signal-regulating kinase 1 (ASK1) and its substrate c-Jun NH<sub>2</sub>-terminal kinase (JNK)<sup>50,51</sup>. JNK phosphorylation has been reported to result in proapoptotic BIM activation and antiapoptotic BCL-2 inhibition.

Many of the pro-death signals from the UPR sensors ultimately converge on the mitochondrial apoptotic pathway, which is triggered when toxic mitochondrial proteins, such as cytochrome c and

Diablo (also known as Smac), are forcibly released into the cytoplasm, which results in activation of downstream effector caspases (for example, caspase-3)<sup>52</sup>. The BCL-2 family proteins govern this 'intrinsic' apoptotic pathway by regulating outer mitochondrial membrane integrity<sup>53</sup>. The intrinsic mitochondrial apoptotic pathway is engaged when cellular damage results in the expression and/or post-translational activation of Bcl-2 homology 3 (BH3)-only proteins, which are a diverse collection of pro-death proteins that contain an  $\alpha$ -helix called the BH3 domain that is necessary for cell death<sup>54</sup>. In the terminal UPR, at least four different BH3-only proteins (BID, BIM, NOXA and PUMA) become activated<sup>55-57</sup>. The mechanism of activation of each BH3-only protein under ER stress is unique. For example, PERK activity leads to transcriptional upregulation of BIM, and the resultant protein product is stabilized by ER stress-dependent JNK dephosphorylation<sup>56</sup>. Once activated, BH3-only proteins disable mitochondrial-protective proteins (for example, BCL-2, BCL-XL and MCL-1) and in some cases directly trigger the multidomain proapoptotic BAX and BAK proteins to permeabilize the outer mitochondrial membrane by a process referred to as mitochondrial outer membrane permeabilization.

### ER stress-related diseases

Cell injury, degeneration and programmed death due to chronic, unmitigated ER stress has been increasingly implicated as underlying the pathophysiology of a wide range of prevalent human diseases<sup>16</sup>. ER stress and sustained UPR signaling have been well documented in affected tissues in diabetes, neurodegeneration, inflammatory disorders, cancer, pulmonary fibrosis and heart disease. In support of the notion that ER stress and maladaptive UPR signaling can contribute to pathology, inherited mutations in the UPR pathway have been associated with rare forms of diabetes and other diseases in humans (see below). For many of the aforementioned diseases, genetic manipulation of specific UPR components has been shown to influence disease outcome in rodent models. A few such diseases most strongly associated with ER stress are discussed below, although more extensive reviews focused on various diseases have been published.

Extensive studies have implicated maladaptive UPR signaling in experimental and common forms of diabetes mellitus. As professional secretory cells, pancreatic  $\beta$  cells synthesize, store and secrete large amounts of the polypeptide hormone insulin; it is estimated that each human  $\beta$  cell produces, on average, about 1 million molecules of insulin every minute to support normoglycemia<sup>8</sup>. Ultimately, this glucostatic cycle is dysregulated in diabetes because the requisite amount of insulin needed to maintain normoglycemia is not produced by a depleted mass of functioning  $\beta$  cells. Myriad rodent models of ER stress-induced  $\beta$ -cell dysfunction (too numerous to list in this Review) amply prove the principle that premature  $\beta$ -cell loss from dysregulated UPR signaling is the causative insult leading to diabetes<sup>8,58</sup>.

Studies have shown that the  $\beta$  cells of mice are most likely operating at UPR activation levels well above those of other professional secretory cells, even in healthy states<sup>59</sup>. Therefore,  $\beta$  cells may readily cross a terminal UPR threshold that puts them at risk for dedifferentiation and apoptosis without having a marked capacity for homeostatic adjustment. Experimental rare diseases may inform our understanding of pathophysiology in common human diabetic syndromes (i.e., types 1 and 2) and eventually lead to target identification for disease modification. Indeed, dysregulation of the PERK and IRE1 $\alpha$  upstream UPR arms has critical consequences for  $\beta$ -cell survival. A striking example of UPR dysregulation in diabetes is evidenced in PERK knockout mice. Massive and rapid  $\beta$ -cell apoptosis, which leads to infantile diabetes, results from homozygous deletion of the *PERK* gene in mice<sup>60,61</sup>. PERK knockout mice also exhibit growth defects and develop pancreatic exocrine insufficiency at early stages of life. These effects are rationalized as being

due to the malfunction and demise of several different types of professional secretory cells, but, interestingly, diabetes mellitus is one of the earliest and most dominant phenotypes in these knockout animals. Intriguingly, *PERK* gene mutations result in a rare human diabetic syndrome (called Wolcott-Rallison syndrome) that is a phenocopy of the mouse *PERK* gene knockout. Furthermore, although homozygous deletion of either *Ire1α* or *Xbp1* impedes embryogenesis and secretory cell development early in embryonic life<sup>23,50,62,63</sup>, the genetic removal of *Xbp1* in the β-cell compartment leads to upstream IRE1α hyperactivation, degeneration of β cells and hyperglycemia, supporting a role for dysregulated IRE1α signaling in ER stress-induced degenerative changes in the endocrine pancreas<sup>64</sup>. Also clearly apparent, the original studies on the *PERK* gene knockout, which leads to diabetes, showed compensatory IRE1α hyperactivation in islets, which may have contributed to degenerative changes in the β-cell compartment as the basis for diabetes progression in addition to the reported mechanism of removing a check on translation<sup>65</sup>.

For various neurodegenerative diseases, a common pathologic hallmark is the accumulation of misfolded proteins and protein aggregates within affected neurons and surrounding supporting cells<sup>66</sup>. Accumulation of many toxic protein species can kill neurons<sup>67</sup>, and there is growing evidence that ER stress is an important mechanism driving this neurotoxicity<sup>68</sup>. IRE1α activation and UPR induction are present in post-mortem brain and spinal cord tissues in Alzheimer's disease<sup>69-71</sup>, Parkinson's disease<sup>72</sup> and amyotrophic lateral sclerosis (ALS)<sup>73</sup>. Moreover, the accumulation of protein aggregates in cellular and animal models of Huntington's disease<sup>51</sup>, Parkinson's disease<sup>74</sup> and ALS<sup>75-77</sup> strongly correlate with UPR activation. Importantly, UPR upregulation is observed before the onset of symptoms, suggesting an active role in the disease<sup>75</sup>. Furthermore, a recent study found that oral administration of a highly selective PERK inhibitor that efficiently crosses the blood-brain barrier reduced neurodegeneration and clinical disease in prion-infected mice<sup>78</sup>.

Finally, we consider the case for UPR modulation in cancers. Tumor cells often invade or metastasize into foreign environments where unfavorable conditions, such as hypoxia, glucose deprivation, lactic acidosis, oxidative stress and inadequate amino acid supplies, compromise protein folding in the ER<sup>79-81</sup>. Indeed, many studies find evidence of sustained and high-level activation of all three branches of the UPR (*PERK*, *ATF6* and *IRE1α*) in a wide range of primary human tumor types, including glioblastoma, multiple myeloma, and carcinomas of the breast, stomach, esophagus and liver<sup>18,82-86</sup>. Also, rare somatic mutations occur in the *Ire1α* gene in a small percentage of human solid tumors<sup>87</sup>. However, despite the overwhelming evidence of ongoing ER stress and UPR activation in many forms of cancer, whether the UPR ultimately inhibits or promotes tumor growth remains unresolved but is an area of active study. Recently, triple-negative breast cancer, an aggressive malignancy

with few treatment options, was found to exhibit a strong XBP1-dependent gene expression signature that correlated with poor prognosis<sup>88</sup>. Myeloma, a highly secretory tumor composed of malignant plasma cells, is another cancer for which the UPR is frequently mentioned as a potentially attractive target on the basis of strong evidence that the UPR, through IRE1α and its homeostatic target XBP1, is essential for plasma cell development<sup>62,63</sup>. Interestingly, up to 50% of primary myelomas show unusually high levels of XBP1s<sup>82</sup>. Moreover, mice expressing a transgene of *Xbp1s* (that is missing the 26-nt intron and hence requires no further processing by IRE1α) in B lymphocytes develop a plasma cell malignancy closely resembling myeloma<sup>82</sup>. There is also evidence to suggest that proteasome inhibition with bortezomib (trade name Velcade), which is approved by the US Food and Drug Administration as first-line therapy for myeloma, leads to myeloma cell death in part by preventing disposal of misfolded proteins through the ERAD pathway and thus triggering ER stress-induced apoptosis<sup>89</sup>. On the basis of these findings,

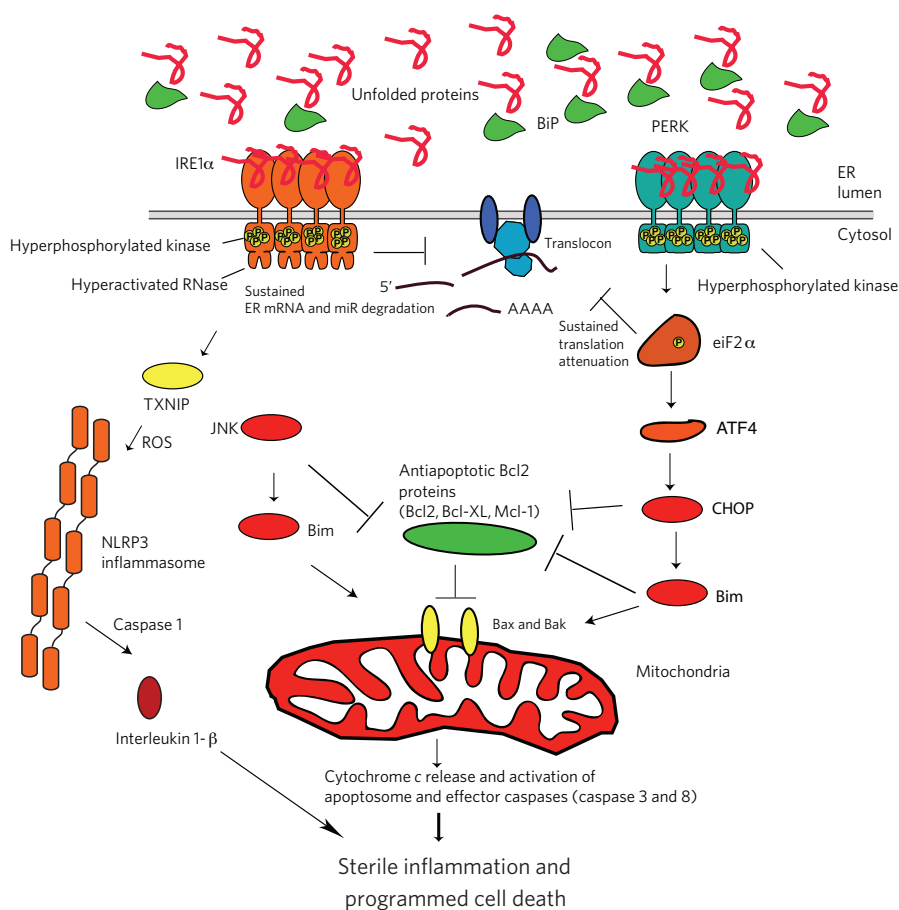


**Figure 4 | Terminal signaling in the UPR.** If ER stress is irremediable, IRE1α becomes hyperactivated and undergoes homo-oligomerization. Under sustained oligomerization, IRE1α's RNase endonucleolytically degrades hundreds of ER-localized mRNAs containing an N-terminal signal sequence, which depletes ER cargo and protein-folding components to further worsen ER stress. Moreover, when hyperactivated, IRE1α's RNase directly cleaves select microRNAs that normally repress proapoptotic targets. In addition to signaling through RNA substrates, IRE1α oligomerization has been shown to induce activation or upregulation of a number of proinflammatory proteins. Finally, sustained IRE1α oligomerization serves as an activation platform for ASK1 and its downstream target JNK. Phosphorylation by JNK has been reported to both activate proapoptotic BIM and inhibit antiapoptotic BCL-2. Though a temporary pause in protein translation due to eIF2α phosphorylation can be beneficial for cells under ER stress, a protracted block in translation from sustained PERK signaling is incompatible with survival. Moreover, high levels of CHOP transcription factor can inhibit the expression of antiapoptotic BCL-2 to hasten cell death and upregulate proapoptotic BIM to trigger activation of the mitochondrial-dependent apoptotic pathway.

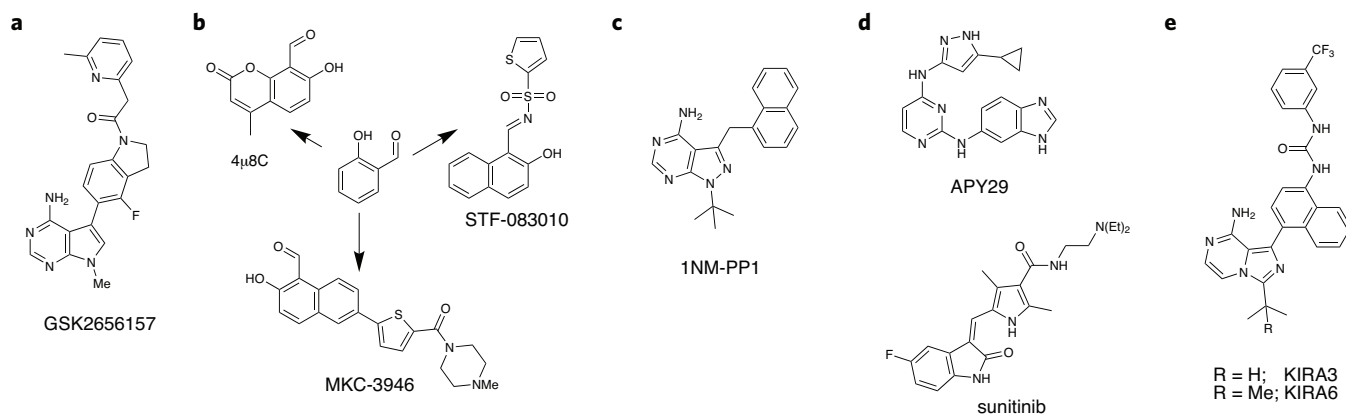


**Figure 5 | Small-molecule modulators of PERK and IRE1 $\alpha$ .** (a) Chemical structure of the ATP-competitive PERK inhibitor GSK2656157.

(b) Salicylaldehyde-based inhibitors of the RNase domain of IRE1 $\alpha$ . (c) Orthogonal type I ATP-competitive inhibitor 1NM-PP1. (d) Type I kinase inhibitors that increase the RNase activity of IRE1 $\alpha$ . (e) Type II kinase inhibitors that inhibit the RNase activity of IRE1 $\alpha$ .

several pharmacologic inhibitors of the IRE1 $\alpha$  RNase activity have recently been tested on human myeloma xenografts and found to have antimyeloma activity<sup>90,91</sup>; however, the specificity and off-target effects of these pharmacological agents are not yet well understood.

Although the above findings suggest an oncogenic role for XBP1s in the development of myeloma, recent data have emerged that challenge this notion. First, downregulation of XBP1s expression in myeloma correlates with resistance to bortezomib<sup>92,93</sup>. Second, using a combination of whole-genome and whole-exome sequencing of primary tumors from 38 myeloma patients, researchers discovered *XBPI* mutations in two of these patients<sup>94</sup>. On further analysis, these mutations were shown to inactivate XBP1s, arguing against an obligate role for this transcription factor in myeloma. Also, arguing against a direct cytoprotective role for IRE1 $\alpha$  in various human cancers, many rare somatic mutations in the *Ire1 $\alpha$*  gene found in glioblastoma, ovarian cancer, lung cancer and gastric cancer encode hypomorphic IRE1 $\alpha$  variants that preserve XBP1 mRNA splicing but prevent the higher-order homo-oligomerization needed to activate extra-XBP1 RNase activity that promotes apoptosis<sup>87,95</sup>. Thus, hypomorphic IRE1 $\alpha$  variants may provide a survival advantage by disabling or coopting the terminal UPR. Furthermore, proliferative blocks through IRE1 $\alpha$  that normally result from ER stress are overcome in the cancer mutants<sup>95</sup>. Finally, it was recently reported that genetic knockdown of IRE1 $\alpha$  or XBP1 in human myeloma cell lines is well tolerated and leads to bortezomib resistance<sup>96</sup>, challenging the rationale for using IRE1 $\alpha$  inhibitors in this disease. Overall, the lessons from myeloma to date suggest that the effects of the UPR (or at least its IRE1 $\alpha$  or XBP1 branches) on tumor development and maintenance are more complicated and nuanced than originally anticipated and that the role of the UPR is perhaps less well understood in cancers than in cell degenerative diseases.

### Pharmacological modulators of IRE1 $\alpha$ and PERK

Does the UPR present tractable drug targets? Given the strong evidence of UPR deregulation across a range of human disease, there is great interest in the possibility of pharmacologically modulating its outputs to control cell fate under ER stress. Pushing the UPR's homeostatic-apoptotic switch toward cell survival could potentially be therapeutically beneficial in cell degenerative diseases such as type 2 diabetes and neurodegeneration. However, the parallel and cross-wired networking of the UPR may require the simultaneous targeting of multiple nodes to obtain desired benefits. One approach may be to lengthen the adaptive phases of the UPR to increase chances of recovery (the transcription factors XBP1 and ATF6 are targets of this kind); such a regime may involve preconditioning the secretory pathway by preemptive UPR activation to make it more

robust. A different approach is to inhibit key mediators of apoptosis (CHOP and TXNIP). Perhaps, potential timers of the UPR such as GADD34 and p58<sup>IPK</sup> may also be appealing targets for intervention. In this vein, a pharmacological agent called salubrinal has been demonstrated to inhibit eIF2 $\alpha$  dephosphorylation and hence result in enhanced cell survival under ER stress<sup>97</sup>.

As previously mentioned, preemptive preconditioning was demonstrated to be partially cytoprotective in cell culture models of ER and oxidative stress using dimerizable versions of PERK in combination with small-molecule dimerizers<sup>39</sup>. However, it is unclear whether the translational inhibition that results from prolonged PERK activation would be efficacious *in vivo*. Related to this, we<sup>45</sup> and others<sup>46</sup> have demonstrated that preemptive activation of IRE1 $\alpha$ 's homeostatic mode using chemical genetics can partially prolong cell survival under ER stress. However, at best, preemptive activation through IRE1 $\alpha$  provides only a small and temporary measure of cytoprotection and furthermore has not been demonstrated to be efficacious in an animal model. Irremediable ER stress hyperactivates both PERK and IRE1 $\alpha$ , leading to entry into apoptosis. Thus, a diametrically opposite strategy is to inhibit the hyperactivated state using inhibitors of PERK<sup>98</sup>, RNase inhibitors of IRE1 $\alpha$ <sup>90</sup> or allosteric RNase-inhibitory type II kinase inhibitors of IRE1 $\alpha$ <sup>34</sup>.

The enzyme active sites of IRE1 $\alpha$  and PERK represent attractive targets for the development of small-molecule modulators of the UPR. Ligands that interact with PERK's kinase domain and IRE1 $\alpha$ 's kinase and RNase domains have been identified (Fig. 5a–e). These small-molecule modulators not only represent promising starting points for the development of therapeutics that target the UPR but also are useful reagents for gaining insight into the functional roles that these multidomain proteins have in responding to ER stress.

**ATP-competitive PERK inhibitors.** Efforts have been made to identify compounds that inhibit the ability of PERK to phosphorylate eIF2 $\alpha$ . Toward this goal, GlaxoSmithKline (GSK) used structure-based design to develop highly potent and selective inhibitors of PERK's kinase domain from an initial screening hit<sup>98</sup>. Optimized ATP-competitive inhibitors, such as GSK2656157, are based on a pyrrolopyrimidine scaffold that displays an indoline-arylacetamide substituent from its C3 position (Fig. 5a). The pyrrolopyrimidine scaffold of GSK2656157 sits in the adenine-binding pocket, and the indoline-arylacetamide moiety projects toward PERK's helix  $\alpha$ C, stabilizing an inactive conformation of this structural element. Helix  $\alpha$ C forms part of the back-to-back dimer interface that the kinase domain of PERK forms, but it is unclear whether the displacement stabilized by GSK2656157 and its analogs disfavor dimerization. In cells, GSK2656157 potently inhibits ER stress-induced PERK

autophosphorylation and the phosphorylation of eIF2 $\alpha$ . This inhibitory activity corresponds to an observed decrease in ATF4 and CHOP. Although early reports suggest that a PERK inhibitor may protect against preclinical models of neurodegeneration<sup>78</sup>, much more work needs to be done to understand the potential benefits and risks of inhibiting ER stress-induced cell degeneration *in vivo*, especially because GSK PERK inhibitors mimic the pancreatic cell loss evident in the mouse Wolcott-Rallison syndrome model (deletion of *Perk* and consequent compensatory activation of IRE1 $\alpha$  in islets).

**Ligands that interact with the RNase domain of IRE1 $\alpha$ .** A number of efforts have been made to identify small molecules that directly inhibit the RNase activity of IRE1 $\alpha$  through its RNase domain<sup>90,91,99,100</sup>. To date, all of the inhibitors identified contain a reactive electrophile that most likely covalently modifies IRE1 $\alpha$ 's RNase active site. The fact that all of these inhibitors contain a reactive moiety is not surprising as the active site of IRE1 $\alpha$ 's RNase is relatively shallow and polar, which presents minimal opportunities for high-affinity interactions with small molecules. The most effective pharmacophore for targeting the RNase domain of IRE1 $\alpha$  has proven to be a salicylaldehyde (Fig. 5b). Inhibitors of this class are exemplified by STF-083010, MKC-3946 and 4 $\mu$ 8c. MKC-3946 and 4 $\mu$ 8c were identified for their abilities to prevent a purified, recombinant kinase-RNase IRE1 $\alpha$  construct from cleaving a fluorescently labeled XBP1 RNA mini-substrate *in vitro*, whereas STF-083010 was a hit in a high-throughput, cell-based reporter gene assay<sup>90,91,99,100</sup>. In cells, inhibitors based on the salicylaldehyde pharmacophore inhibit the RNase activity of IRE1 $\alpha$  without affecting its ability to autophosphorylate. Presumably, these inhibitors also do not prevent IRE1 $\alpha$  dimerization and oligomerization under ER stress.

The similar potencies of structurally diverse salicylaldehyde-based inhibitors suggests that the efficacy of these compounds is most likely driven by reactivity more than binding affinity. Indeed, the half-maximum inhibitory concentration values of STF-083010, MKC-3946 and 4 $\mu$ 8c are within 10- to 20-fold of one another in *in vitro* RNase activity assays. Several studies have shown that salicylaldehyde-based inhibitors form a Schiff base with a lysine in the RNase active site<sup>100,101</sup>. As other salicylaldehyde-based inhibitors compete with 4 $\mu$ 8c for Schiff base formation, it is likely that lysine 907 is generally targeted by this inhibitor class. Several

recently reported crystal structures of murine IRE1 $\alpha$  bound to salicylaldehyde-based inhibitors show that lysine 907 is indeed involved in Schiff base formation<sup>101</sup>. Furthermore, these structural studies provide insight into how covalent bond formation interferes with RNase activity.

**Ligands that interact with the kinase domain of IRE1 $\alpha$ .** Several ATP-competitive inhibitors that target the kinase domain of IRE1 $\alpha$  have been identified. Although all of these ligands inhibit the kinase activity of IRE1 $\alpha$ , occupation of the ATP-binding site can have profoundly divergent effects on the RNase domain. Allosteric communication between the ATP-binding site and RNase domain was first discovered in a yeast IRE1 mutant that contains an enlarged ('holed') ATP-binding pocket, which can be selectively complemented with the orthogonal type I ATP-competitive inhibitor 1NM-PP1 (Fig. 5c)<sup>47</sup>. Holed ATP-binding site mutants of IRE1 have crippled kinase and RNase activities, but binding of 1NM-PP1 to IRE1's ATP-binding site restores RNase function. Thus, an ATP-competitive ligand is able to allosterically activate IRE1's RNase domain in the absence of kinase autophosphorylation. This allosteric relationship is maintained in human IRE1 $\alpha$ , as 1NM-PP1 is able to restore holed human IRE1 $\alpha$ 's ability to cleave RNA *in vitro* and in cells. ATP-competitive inhibitors of wild-type IRE1 $\alpha$  are also able to activate RNase activity while inhibiting kinase activity. For example, the promiscuous ATP-competitive inhibitor APY29 and the clinically approved drug sunitinib activate IRE1 $\alpha$ 's RNase domain (Fig. 5d)<sup>34,35,43</sup>. In addition, these ATP-competitive inhibitors increase the dimerization or oligomerization state of IRE1 $\alpha$ , which most likely contributes to the observed enhancement of RNase activity.

Recently, ATP-competitive ligands that inhibit IRE1 $\alpha$ 's RNase activity through the kinase domain have been identified (Fig. 5e)<sup>34</sup>. These kinase-inhibiting RNase attenuators (KIRAs) were discovered by screening type II ATP-competitive ligands, which stabilize inactive ATP-binding site conformations, for their abilities to block the RNase activity of a recombinant IRE1 $\alpha$  kinase-RNase construct. Optimization of an initial hit based on a pyrazolopyrimidine scaffold resulted in KIRA3 (Fig. 5e), which inhibits the kinase and RNase activities of IRE1 $\alpha$  *in vitro* and in cells. Consistent with its divergent behavior relative to type I ATP-competitive inhibitors, KIRA3 directly opposes the ability of APY29 to activate the RNase domain of IRE1 $\alpha$ . Furthermore, and in contrast to sunitinib and APY29, KIRA3 suppresses the dimerization-oligomerization

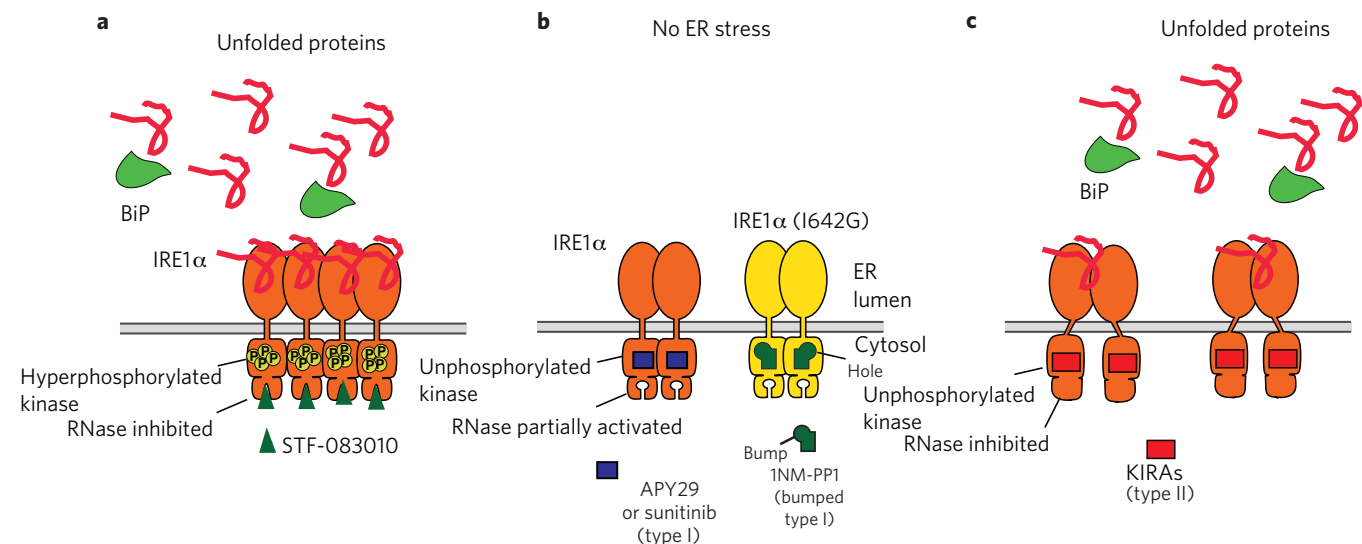


**Figure 6 | Modes of pharmacological modulation of IRE1 $\alpha$ .** (a) Model of how salicylaldehyde-based RNase inhibitors affect intracellular IRE1 $\alpha$ . (b) Model of how type I kinase inhibitors affect intra-cellular IRE1 $\alpha$ . (c) Model of how type II kinase inhibitors affect intracellular IRE1 $\alpha$ .

of IRE1 $\alpha$  by stabilizing the monomeric form of this protein. Although a structure of KIRA3 bound to IRE1 $\alpha$  has not yet been determined, stabilization of an inactive, ATP-binding site conformation most likely leads to stabilization of monomeric IRE1 $\alpha$  and suppression of RNase inhibition.

A more advanced KIRA, KIRA6 (Fig. 5e), with suitable pharmacokinetic properties for *in vivo* studies, showed greater potency and dose-dependently reduced IRE1 $\alpha$  phosphorylation, oligomerization and RNase activation *in vitro* and *in vivo* to preserve both cell viability and function. Importantly, KIRA6 showed efficacy in two different animal models of ER stress-induced cell degeneration: Specifically, KIRA6 preserved photoreceptor functional viability in rat models of ER stress-induced retinal degeneration when injected into the vitreous. Moreover, KIRA6 preserved pancreatic  $\beta$  cells, increased insulin and reduced hyperglycemia in Akita diabetic mice, which spontaneously develop diabetes in neonatal life because they harbor a mutant proinsulin that is unable to complete oxidative folding, resulting in chronic ER stress and  $\beta$ -cell apoptosis<sup>49,95</sup>.

The availability of diverse ligands that target two distinct active sites presents unique opportunities to pharmacologically tune the intracellular behavior of IRE1 $\alpha$ , perhaps even combinatorially<sup>95</sup>. Under ER stress, salicylaldehyde-based inhibitors will directly inhibit the RNase activity of IRE1 $\alpha$  but not prevent autophosphorylation or the phosphorylation of any potential nonautonomous protein substrates (Fig. 6a). Furthermore, direct inhibition of the RNase domain most likely does not prevent dimerization or oligomerization. Type I inhibitors, such as APY29 and sunitinib, will prevent IRE1 $\alpha$  autophosphorylation but activate the RNase domain, even in the absence of ER stress (Fig. 6b). Furthermore, inhibitors of this class should enhance IRE1 $\alpha$  dimerization or oligomerization. In contrast, type II inhibitors, such as KIRA3 and KIRA6, inhibit both the kinase and RNase activities of IRE1 $\alpha$  (Fig. 6c). Additionally, type II IRE1 $\alpha$  inhibitors will stabilize the monomeric form and oppose dimerization or oligomerization induced by ER stress.

## Conclusions

The UPR is a highly conserved signaling pathway that is activated when cells are not able to keep pace with the protein folding demands of the ER—a form of cell injury called ER stress. Under ER stress, the UPR initially sends out adaptive outputs that reduce the protein-folding load and expand the capacity of the ER secretory pathway. However, under irremediable ER stress, the UPR assembles into a platform that sends out proinflammatory and pro-death signals to cause cell demise. Cell injury from chronic ER stress is emerging as central to the pathophysiology of a wide range of prevalent human diseases, including diabetes, neurodegeneration, stroke and cancer. Recent advances in our understanding of how the UPR switches from life to death signaling may lead to new strategies to combat these ER stress-associated diseases. In this regard, the recent findings from many research groups, which (i) demonstrate that two master regulators of the UPR, PERK and IRE1 $\alpha$ , akin to cell surface death receptors, have binary outputs promoting either life or death decisions for the ER-stressed cell and (ii) identify new small-molecule modulators of these proteins, offer rich opportunities to dissect the contribution of these signaling proteins to pathogenesis in myriad models of human ER stress-related diseases. As such, future studies will be enabled by optimizing compounds directed toward these master UPR regulators to determine whether PERK and IRE1 $\alpha$  are viable targets for disease modification, and may serve as starting points for a first-in-class series of drugs. Furthermore, the combined application of PERK and IRE1 $\alpha$  inhibitors may prevent compensatory activation resulting from inhibition of either kinase in isolation. Thus, combination therapy against the two druggable kinases of the UPR may emerge someday as a useful means to ameliorate the critical downstream terminal signaling

events that are linked to cell demise in myriad diseases proceeding from unchecked ER stress.

Received 17 June 2014; accepted 15 September 2014; published online 17 October 2014

- Anelli, T. & Sitia, R. Protein quality control in the early secretory pathway. *EMBO J.* **27**, 315–327 (2008)
- Tu, B.P. & Weissman, J.S. Oxidative protein folding in eukaryotes: mechanisms and consequences. *J. Cell Biol.* **164**, 341–346 (2004)
- Sevier, C.S. & Kaiser, C.A. Formation and transfer of disulphide bonds in living cells. *Nat. Rev. Mol. Cell Biol.* **3**, 836–847 (2002)
- van Anken, E. & Braakman, I. Versatility of the endoplasmic reticulum protein folding factory. *Crit. Rev. Biochem. Mol. Biol.* **40**, 191–228 (2005)
- Merksamer, P.I., Trusina, A. & Papa, F.R. Real-time redox measurements during endoplasmic reticulum stress reveal interlinked protein folding functions. *Cell* **135**, 933–947 (2008)
- Smith, M.H., Ploegh, H.L. & Weissman, J.S. Road to ruin: targeting proteins for degradation in the endoplasmic reticulum. *Science* **334**, 1086–1090 (2011)
- Meusser, B., Hirsch, C., Jarosch, E. & Sommer, T. ERAD: the long road to destruction. *Nat. Cell Biol.* **7**, 766–772 (2005)
- Scheuner, D. & Kaufman, R.J. The unfolded protein response: a pathway that links insulin demand with  $\beta$ -cell failure and diabetes. *Endocr. Rev.* **29**, 317–333 (2008)
- van Anken, E. *et al.* Efficient IgM assembly and secretion require the plasma cell induced endoplasmic reticulum protein pERp1. *Proc. Natl. Acad. Sci. USA* **106**, 17019–17024 (2009)
- Tabas, I. & Ron, D. Integrating the mechanisms of apoptosis induced by endoplasmic reticulum stress. *Nat. Cell Biol.* **13**, 184–190 (2011)
- Oyadomari, S. *et al.* Targeted disruption of the *Chop* gene delays endoplasmic reticulum stress-mediated diabetes. *J. Clin. Invest.* **109**, 525–532 (2002)
- Zhang, H.M. *et al.* Coxsackievirus B3 infection activates the unfolded protein response and induces apoptosis through downregulation of p58IPK and activation of CHOP and SREBP1. *J. Virol.* **84**, 8446–8459 (2010)
- Ma, Y. & Hendershot, L.M. ER chaperone functions during normal and stress conditions. *J. Chem. Neuroanat.* **28**, 51–65 (2004)
- Flamment, M., Hajdich, E., Ferre, P. & Foufelle, F. New insights into ER stress-induced insulin resistance. *Trends Endocrinol. Metab.* **23**, 381–390 (2012)
- Gestwicki, J.E. & Garza, D. Protein quality control in neurodegenerative disease. *Prog. Mol. Biol. Transl. Sci.* **107**, 327–353 (2012)
- Wang, S. & Kaufman, R.J. The impact of the unfolded protein response on human disease. *J. Cell Biol.* **197**, 857–867 (2012)
- Pincus, D. *et al.* BiP binding to the ER-stress sensor Ire1 tunes the homeostatic behavior of the unfolded protein response. *PLoS Biol.* **8**, e1000415 (2010)
- Gardner, B.M. & Walter, P. Unfolded proteins are Ire1-activating ligands that directly induce the unfolded protein response. *Science* **333**, 1891–1894 (2011)
- Credle, J.J., Finer-Moore, J.S. & Papa, F.R. Stroud, R. M. & Walter, P. On the mechanism of sensing unfolded protein in the endoplasmic reticulum. *Proc. Natl. Acad. Sci. USA* **102**, 18773–18784 (2005)
- Walter, P. & Ron, D. The unfolded protein response: from stress pathway to homeostatic regulation. *Science* **334**, 1081–1086 (2011)
- Travers, K.J. *et al.* Functional and genomic analyses reveal an essential coordination between the unfolded protein response and ER-associated degradation. *Cell* **101**, 249–258 (2000)
- Harding, H.P., Zhang, Y. & Ron, D. Protein translation and folding are coupled by an endoplasmic-reticulum-resident kinase. *Nature* **397**, 271–274 (1999)
- Tirasophon, W., Welihinda, A.A. & Kaufman, R.J. A stress response pathway from the endoplasmic reticulum to the nucleus requires a novel bifunctional protein kinase/endoribonuclease (Ire1p) in mammalian cells. *Genes Dev.* **12**, 1812–1824 (1998)
- Wang, X.Z. *et al.* Cloning of mammalian Ire1 reveals diversity in the ER stress responses. *EMBO J.* **17**, 5708–5717 (1998)
- Korennykh, A. & Walter, P. Structural basis of the unfolded protein response. *Annu. Rev. Cell Dev. Biol.* **28**, 251–277 (2012)
- Calton, M. *et al.* IRE1 couples endoplasmic reticulum load to secretory capacity by processing the XBP-1 mRNA. *Nature* **415**, 92–96 (2002)
- Yoshida, H., Matsui, T., Yamamoto, A., Okada, T. & Mori, K. XBP1 mRNA is induced by ATF6 and spliced by IRE1 in response to ER stress to produce a highly active transcription factor. *Cell* **107**, 881–891 (2001)
- Yamamoto, K. *et al.* Transcriptional induction of mammalian ER quality control proteins is mediated by single or combined action of ATF6a and XBP1. *Dev. Cell* **13**, 365–376 (2007)
- Liu, C.Y., Schroder, M. & Kaufman, R.J. Ligand-independent dimerization activates the stress response kinases IRE1 and PERK in the lumen of the endoplasmic reticulum. *J. Biol. Chem.* **275**, 24881–24885 (2000)
- Bertolotti, A., Zhang, Y., Hendershot, L.M., Harding, H.P. & Ron, D. Dynamic interaction of BiP and ER stress transducers in the unfolded-protein response. *Nat. Cell Biol.* **2**, 326–332 (2000)



31. Harding, H.P. *et al.* An integrated stress response regulates amino acid metabolism and resistance to oxidative stress. *Mol. Cell* **11**, 619–633 (2003)
32. Ye, J. *et al.* ER stress induces cleavage of membrane-bound ATF6 by the same proteases that process SREBPs. *Mol. Cell* **6**, 1355–1364 (2000)
33. Lee, K.P. *et al.* Structure of the dual enzyme Ire1 reveals the basis for catalysis and regulation in nonconventional RNA splicing. *Cell* **132**, 89–100 (2008)  
**The first crystal structure of the kinase-RNase portion of IRE1. This paper provides a model for how back-to-back dimerization leads to RNase activation.**
34. Wang, L. *et al.* Divergent allosteric control of the IRE1 $\alpha$  endoribonuclease using kinase inhibitors. *Nat. Chem. Biol.* **8**, 982–989 (2012)  
**This manuscript demonstrates that it is possible to allosterically inhibit IRE1 $\alpha$ 's RNase activity through its kinase domain with a conformation-selective ATP-competitive ligand.**
35. Korennykh, A.V. *et al.* The unfolded protein response signals through high-order assembly of Ire1. *Nature* **457**, 687–693 (2009)  
**This study demonstrates that the cytosolic portion of baker's yeast IRE1 is capable of forming an ordered rod-shaped oligomer. The crystal structure of this higher-order assembly and accompanying biophysical studies provide a mechanistic model linking IRE1 autophosphorylation to its RNase activity.**
36. Korennykh, A.V. *et al.* Cofactor-mediated conformational control in the bifunctional kinase/RNase Ire1. *BMC Biol.* **9**, 48 (2011)
37. Ali, M.M. *et al.* Structure of the Ire1 autophosphorylation complex and implications for the unfolded protein response. *EMBO J.* **30**, 894–905 (2011)
38. Shore, G.C., Papa, F.R. & Oakes, S.A. Signaling cell death from the endoplasmic reticulum stress response. *Curr. Opin. Cell Biol.* **23**, 143–149 (2011)
39. Lu, P.D. *et al.* Cytoprotection by pre-emptive conditional phosphorylation of translation initiation factor 2. *EMBO J.* **23**, 169–179 (2004)
40. Lin, J.H., Li, H., Zhang, Y., Ron, D. & Walter, P. Divergent effects of PERK and IRE1 signaling on cell viability. *PLoS ONE* **4**, e4170 (2009)
41. McCullough, K.D., Martindale, J.L., Klotz, L.O., Aw, T.Y. & Holbrook, N.J. Gadd153 sensitizes cells to endoplasmic reticulum stress by down-regulating Bcl2 and perturbing the cellular redox state. *Mol. Cell Biol.* **21**, 1249–1259 (2001)
42. Marciniak, S.J. *et al.* CHOP induces death by promoting protein synthesis and oxidation in the stressed endoplasmic reticulum. *Genes Dev.* **18**, 3066–3077 (2004)
43. Han, D. *et al.* IRE1 $\alpha$  kinase activation modes control alternate endoribonuclease outputs to determine divergent cell fates. *Cell* **138**, 562–575 (2009)  
**This manuscript showed that endonucleolytic decay of ER-localized mRNAs by IRE1 $\alpha$  is linked to apoptosis. Furthermore, it showed that adaptive XBP1 mRNA splicing can be uncoupled from proapoptotic extra-XBP1 mRNA decay using INM-PP1-sensitized IRE1 $\alpha$ .**
44. Hollien, J. & Weissman, J.S. Decay of endoplasmic reticulum-localized mRNAs during the unfolded protein response. *Science* **313**, 104–107 (2006)
45. Han, D. *et al.* A kinase inhibitor activates the IRE1 $\alpha$  RNase to confer cytoprotection against ER stress. *Biochem. Biophys. Res. Commun.* **365**, 777–783 (2008)
46. Lin, J.H. *et al.* IRE1 signaling affects cell fate during the unfolded protein response. *Science* **318**, 944–949 (2007)
47. Papa, F.R., Zhang, C., Shokat, K. & Walter, P. Bypassing a kinase activity with an ATP-competitive drug. *Science* **302**, 1533–1537 (2003)  
**The first demonstration of the allosteric relationship between the kinase and RNase domains of IRE1. The authors found that an ATP-competitive inhibitor is able to activate IRE1's RNase domain in the absence of autophosphorylation.**
48. Upton, J.P. *et al.* IRE1 $\alpha$  cleaves select microRNAs during ER stress to derepress translation of proapoptotic Caspase-2. *Science* **338**, 818–822 (2012)
49. Lerner, A.G. *et al.* IRE1 $\alpha$  induces thioredoxin-interacting protein to activate the NLRP3 inflammasome and promote programmed cell death under irremediable ER stress. *Cell Metab.* **16**, 250–264 (2012)
50. Urano, F. *et al.* Coupling of stress in the ER to activation of JNK protein kinases by transmembrane protein kinase IRE1. *Science* **287**, 664–666 (2000)
51. Nishitoh, H. *et al.* ASK1 is essential for endoplasmic reticulum stress-induced neuronal cell death triggered by expanded polyglutamine repeats. *Genes Dev.* **16**, 1345–1355 (2002)
52. Wang, C. & Youle, R.J. The role of mitochondria in apoptosis. *Annu. Rev. Genet.* **43**, 95–118 (2009)
53. Chipuk, J.E., Moldoveanu, T., Llambi, F., Parsons, M.J. & Green, D.R. The BCL-2 family reunion. *Mol. Cell* **37**, 299–310 (2010)
54. Giam, M., Huang, D.C. & Bouillet, P. BH3-only proteins and their roles in programmed cell death. *Oncogene* **27**, Suppl 1, S128–S136 (2008)
55. Upton, J.P. *et al.* Caspase-2 cleavage of BID is a critical apoptotic signal downstream of endoplasmic reticulum stress. *Mol. Cell Biol.* **28**, 3943–3951 (2008)
56. Puthalakath, H. *et al.* ER stress triggers apoptosis by activating BH3-only protein Bim. *Cell* **129**, 1337–1349 (2007)
57. Li, J., Lee, B. & Lee, A.S. Endoplasmic reticulum stress-induced apoptosis: multiple pathways and activation of p53-up-regulated modulator of apoptosis (PUMA) and NOXA by p53. *J. Biol. Chem.* **281**, 7260–7270 (2006)
58. Papa, F.R. Endoplasmic reticulum stress, pancreatic b-cell degeneration, and diabetes. *Cold Spring Harb. Perspect. Med.* **2**, a007666 (2012)
59. Iwawaki, T., Akai, R., Kohno, K. & Miura, M. A transgenic mouse model for monitoring endoplasmic reticulum stress. *Nat. Med.* **10**, 98–102 (2004)
60. Harding, H.P., Zhang, Y., Bertolotti, A., Zeng, H. & Ron, D. Perk is essential for translational regulation and cell survival during the unfolded protein response. *Mol. Cell* **5**, 897–904 (2000)
61. Delépine, M. *et al.* EIF2AK3, encoding translation initiation factor 2- $\alpha$  kinase 3, is mutated in patients with Wolcott-Rallison syndrome. *Nat. Genet.* **25**, 406–409 (2000)
62. Reimold, A.M. *et al.* Plasma cell differentiation requires the transcription factor XBP-1. *Nature* **412**, 300–307 (2001)
63. Zhang, K. *et al.* The unfolded protein response sensor IRE1 $\alpha$  is required at 2 distinct steps in B cell lymphopoiesis. *J. Clin. Invest.* **115**, 268–281 (2005)
64. Lee, A.H., Heidtman, K., Hotamisligil, G.S. & Glimcher, L.H. Dual and opposing roles of the unfolded protein response regulated by IRE1 $\alpha$  and XBP1 in proinsulin processing and insulin secretion. *Proc. Natl. Acad. Sci. USA* **108**, 8885 (2011)  
**This manuscript showed that Xbp1 gene deletion in  $\beta$  cells of the endocrine pancreas caused compensatory IRE1 $\alpha$  hyperactivation, leading to endonucleolytic decay of a number of ER-localized mRNAs that are normally needed to maintain  $\beta$  cell-differentiated identity and the ability to process and secrete insulin.**
65. Harding, H.P. *et al.* Diabetes mellitus and exocrine pancreatic dysfunction in *Perk*<sup>-/-</sup> mice reveals a role for translational control in secretory cell survival. *Mol. Cell* **7**, 1153–1163 (2001)  
**This manuscript showed that homozygous *Perk* gene deletion causes degeneration of several professional secretory tissues, including a cells of the endocrine pancreas, consequently leading to diabetes. Pancreatic islets of *Perk*<sup>-/-</sup> mice demonstrated decreased translational attenuation and compensatory IRE1 $\alpha$  hyperactivation at baseline.**
66. Ross, C.A. & Poirier, M.A. Protein aggregation and neurodegenerative disease. *Nat. Med.* **10**, S10–S17 (2004)
67. Taylor, J.P., Hardy, J. & Fischbeck, K.H. Toxic proteins in neurodegenerative disease. *Science* **296**, 1991–1995 (1991).
68. Roussel, B.D. *et al.* Endoplasmic reticulum dysfunction in neurological disease. *Lancet Neurol.* **12**, 105–118 (2013)
69. Hamos, J.E. *et al.* Expression of heat shock proteins in Alzheimer's disease. *Neurology* **41**, 345–350 (1991)
70. Hoozemans, J.J. *et al.* The unfolded protein response is activated in pretangle neurons in Alzheimer's disease hippocampus. *Am. J. Pathol.* **174**, 1241–1251 (2009)
71. Unterberger, U. *et al.* Endoplasmic reticulum stress features are prominent in Alzheimer disease but not in prion diseases *in vivo*. *J. Neuropathol. Exp. Neurol.* **65**, 348–357 (2006)
72. Wang, H.Q. & Takahashi, R. Expanding insights on the involvement of endoplasmic reticulum stress in Parkinson's disease. *Antioxid. Redox Signal.* **9**, 553–561 (2007)
73. Atkin, J.D. *et al.* Endoplasmic reticulum stress and induction of the unfolded protein response in human sporadic amyotrophic lateral sclerosis. *Neurobiol. Dis.* **30**, 400–407 (2008)
74. Holtz, W.A. & O'Malley, K.L. Parkinsonian mimetics induce aspects of unfolded protein response in death of dopaminergic neurons. *J. Biol. Chem.* **278**, 19367–19377 (2003)
75. Atkin, J.D. *et al.* Induction of the unfolded protein response in familial amyotrophic lateral sclerosis and association of protein-disulfide isomerase with superoxide dismutase 1. *J. Biol. Chem.* **281**, 30152–30165 (2006)
76. Kikuchi, H. *et al.* Spinal cord endoplasmic reticulum stress associated with a microsomal accumulation of mutant superoxide dismutase-1 in an ALS model. *Proc. Natl. Acad. Sci. USA* **103**, 6025–6030 (2006)
77. Nishitoh, H. *et al.* ALS-linked mutant SOD1 induces ER stress- and ASK1-dependent motor neuron death by targeting Derlin-1. *Genes Dev.* **22**, 1451–1464 (2008)
78. Moreno, J. A. *et al.* Oral treatment targeting the unfolded protein response prevents neurodegeneration and clinical disease in prion-infected mice. *Sci. Transl. Med.* **5**, 206ra138 (2013).  
**This work showed that prion protein replication hyperactivates the UPR, leading to neuronal death. PERK inhibitors attenuated translational shutdown and reduced clinical prion disease in rodents.**
79. Lee, A.S. & Hendershot, L.M. ER stress and cancer. *Cancer Biol. Ther.* **5**, 721–722 (2006)
80. Koumenis, C. ER stress, hypoxia tolerance and tumor progression. *Curr. Mol. Med.* **6**, 55–69 (2006)
81. Moenner, M., Pluquet, O., Bouchecareilh, M. & Chevet, E. Integrated endoplasmic reticulum stress responses in cancer. *Cancer Res.* **67**, 10631–10634 (2007)

82. Carrasco, D.R. *et al.* The differentiation and stress response factor XBP-1 drives multiple myeloma pathogenesis. *Cancer Cell* **11**, 349–360 (2007)
83. Fernandez, P.M. *et al.* Overexpression of the glucose-regulated stress gene GRP78 in malignant but not benign human breast lesions. *Breast Cancer Res. Treat.* **59**, 15–26 (2000)
84. Shuda, M. *et al.* Activation of the *ATF6*, *XBP1* and *grp78* genes in human hepatocellular carcinoma: a possible involvement of the ER stress pathway in hepatocarcinogenesis. *J. Hepatol.* **38**, 605–614 (2003)
85. Song, M.S., Park, Y.K., Lee, J.H. & Park, K. Induction of glucose-regulated protein 78 by chronic hypoxia in human gastric tumor cells through a protein kinase C-e/ERK/AP-1 signaling cascade. *Cancer Res.* **61**, 8322–8330 (2001).
86. Chen, X., Ding, Y., Liu, C.G., Mikhail, S. & Yang, C.S. Overexpression of glucose-regulated protein 94 (Grp94) in esophageal adenocarcinomas of a rat surgical model and humans. *Carcinogenesis* **23**, 123–130 (2002)
87. Greenman, C. *et al.* Patterns of somatic mutation in human cancer genomes. *Nature* **446**, 153–158 (2007)
88. Chen, X. *et al.* XBP1 promotes triple-negative breast cancer by controlling the HIF1 $\alpha$  pathway. *Nature* **508**, 103–107 (2014)
89. Voorhees, P.M. & Orlowski, R.Z. The proteasome and proteasome inhibitors in cancer therapy. *Annu. Rev. Pharmacol. Toxicol.* **46**, 189–213 (2006)
90. Papandreou, I. *et al.* Identification of an Ire1 $\alpha$  endonuclease specific inhibitor with cytotoxic activity against human multiple myeloma. *Blood* **117**, 1311–1314 (2011)
91. Mimura, N. *et al.* Blockade of XBP1 splicing by inhibition of Ire1 $\alpha$  is a promising therapeutic option in multiple myeloma. *Blood* **119**, 5772–5781 (2012)
92. Gu, J.L. *et al.* Differentiation induction enhances bortezomib efficacy and overcomes drug resistance in multiple myeloma. *Biochem. Biophys. Res. Commun.* **420**, 644–650 (2012)
93. Ling, S.C. *et al.* Response of myeloma to the proteasome inhibitor bortezomib is correlated with the unfolded protein response regulator XBP-1. *Haematologica* **97**, 64–72 (2012)
94. Chapman, M.A. *et al.* Initial genome sequencing and analysis of multiple myeloma. *Nature* **471**, 467–472 (2011)
95. Ghosh, R. *et al.* Allosteric inhibition of the Ire1 $\alpha$  RNase preserves cell viability and function during endoplasmic reticulum stress. *Cell* **158**, 534–548 (2014)
- This manuscript showed that the Ire1 $\alpha$  kinase rheostatically activates the Ire1 $\alpha$  RNase domain through self-association, leading to apoptosis past an oligomerization threshold. Furthermore, KIRAs of Ire1 $\alpha$  reduce homo-**
- oligomerization, terminal UPR signaling and apoptosis under ER stress; in two animal models of ER stress-induced cell loss, an advanced KIRA, KIRA6, showed therapeutic benefits.**
96. Leung-Hagesteijn, C. *et al.* Xbp1s-negative tumor B cells and pre-plasmablasts mediate therapeutic proteasome inhibitor resistance in multiple myeloma. *Cancer Cell* **24**, 289–304 (2013)
97. Boyce, M. *et al.* A selective inhibitor of eIF2 $\alpha$  dephosphorylation protects cells from ER stress. *Science* **307**, 935–939 (2005)
98. Atkins, C. *et al.* Characterization of a novel PERK kinase inhibitor with antitumor and antiangiogenic activity. *Cancer Res.* **73**, 1993–2002 (2013)
- This paper describes the identification of the first-in-class ATP-competitive PERK inhibitor GSK2656157. The authors demonstrate that this potent and selective compound leads to reduced ATF4 and CHOP levels in multiple cell lines and growth inhibition in several tumor xenografts.**
99. Volkmann, K. *et al.* Potent and selective inhibitors of the inositol-requiring enzyme 1 endoribonuclease. *J. Biol. Chem.* **286**, 12743–12755 (2011)
100. Cross, B.C. *et al.* The molecular basis for selective inhibition of unconventional mRNA splicing by an Ire1-binding small molecule. *Proc. Natl. Acad. Sci. USA* **109**, E869–E878 (2012)
101. Sanches, M. *et al.* Structure and mechanism of action of the hydroxy-aryl-aldehyde class of Ire1 endoribonuclease inhibitors. *Nat. Commun.* **5**, 4202 (2014)

### Acknowledgments

This work was supported by the US National Institutes of Health grants DP2OD001925 (F.R.P.), RO1DK080955 (F.R.P.), P30DK063720 (F.R.P.), UO1DK089541 (F.R.P.), RO1DK100623 (F.R.P. and D.J.M.), R01GM086858 (D.J.M.); the Burroughs Wellcome Foundation (F.R.P.); the Juvenile Diabetes Research Foundation (F.R.P.); the Harrington Discovery Institute Scholar-Innovator Award (F.R.P.); the Alfred P. Sloan Foundation (D.J.M.); and the Camille and Henry Dreyfus Foundation (D.J.M.).

### Competing financial interests

The authors declare no competing financial interests.

### Additional information

Reprints and permissions information is available online at <http://www.nature.com/reprints/index.html>. Correspondence and requests for materials should be addressed to D.J.M. or F.R.P.